The Journal of Physical Chemistry Letters
Letter
Cite This: J. Phys. Chem. Lett. 2018, 9, 2620−2626
pubs.acs.org/JPCL

VUV Photoionization Study of the Formation of the Simplest Polycyclic Aromatic Hydrocarbon: Naphthalene ($C_{10}H_8$)

Long Zhao and Ralf I. Kaiser*

Department of Chemistry, University of Hawaii at Manoa, Honolulu, Hawaii 96822, United States

Bo Xu, Utuq Ablikim, and Musahid Ahmed*

Chemical Sciences Division, Lawrence Berkeley National Laboratory, Berkeley, California 94720, United States

Marsel V. Zagidullin and Valeriy N. Azyazov

Samara National Research University, Samara 443086, Russia
Lebedev Physical Institute, Samara 443011, Russia

A. Hasan Howlader and Stanislaw F. Wnuk

Department of Chemistry and Biochemistry, Florida International University, Miami, Florida 33199, United States

Alexander M. Mebel*

Department of Chemistry and Biochemistry, Florida International University, Miami, Florida 33199, United States
Samara National Research University, Samara 443086, Russia

Supporting Information

ABSTRACT: The formation of the simplest polycyclic aromatic hydrocarbon (PAH), naphthalene ($C_{10}H_8$), was explored in a high-temperature chemical reactor under combustion-like conditions in the phenyl (C_6H_5)−vinylacetylene (C_4H_4) system. The products were probed utilizing tunable vacuum ultraviolet light by scanning the photoionization efficiency (PIE) curve at a mass-to-charge $m/z = 128$ ($C_{10}H_8^+$) of molecules entrained in a molecular beam. The data fitting with PIE reference curves of naphthalene, 4-phenylvinylacetylene ($C_6H_5CCC_2H_3$), and *trans*-1-phenylvinylacetylene ($C_6H_5CHCHCCH$) indicates that the isomers were generated with branching ratios of 43.5±9.0 : 6.5±1.0 : 50.0±10.0%. Kinetics simulations agree nicely with the experimental findings with naphthalene synthesized via the hydrogen abstraction−vinylacetylene addition (HAVA) pathway and through hydrogen-assisted isomerization of phenylvinylacetylenes. The HAVA route to naphthalene at elevated temperatures represents an alternative pathway to the hydrogen abstraction−acetylene addition (HACA) forming naphthalene in flames and circumstellar envelopes, whereas in cold molecular clouds, HAVA synthesizes naphthalene via a barrierless bimolecular route.

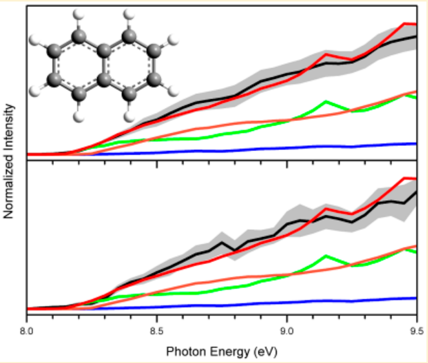

Polycyclic aromatic hydrocarbons (PAHs), organic molecules consisting of fused benzene rings, along with their protonated, ionized, (de)hydrogenated, alkylated, and nitrogen-substituted counterparts, have been proposed to carry up to 20% of the interstellar carbon budget. Inferred from the diffuse interstellar bands (DIBs),[1,2] discrete absorption features superimposed on the interstellar extinction curve covering the blue part of the visible spectrum (400 nm) to the near-infrared (1.2 μm), and from the unidentified infrared (UIR) emission bands monitored from 3 to 14 μm,[3,4] PAHs have been linked to the astrobiological evolution of the interstellar medium[5] and are contemplated as key nucleation sites leading to carbonaceous dust particles ("interstellar grains").[6−11] Even though not a single PAH has been observed spectroscopically in the gas phase of the interstellar medium (ISM), the identification of the

Received: April 3, 2018
Accepted: May 2, 2018
Published: May 2, 2018

DOI: 10.1021/acs.jpclett.8b01020
J. Phys. Chem. Lett. 2018, 9, 2620−2626

prototype PAH naphthalene ($C_{10}H_8$) along with higher-molecular-weight PAHs like coronene ($C_{24}H_{12}$) in at least 20 carbonaceous chondrites proposes a circumstellar origin around envelopes of dying Asymptotic Giant Branch (AGB) stars.[12,13] State-of-the-art astrochemical models of PAH formation have been "borrowed" from the combustion chemistry community with the most commended pathways to PAHs proposed to be associated with molecular-weight growth processes via sequential reactions of resonantly stabilized (propargyl; C_3H_3) and also aromatic (phenyl; C_6H_5) radicals. Together with acetylene (C_2H_2), these reactions are contemplated as the foundation for the hydrogen abstraction−acetylene addition (HACA) mechanism[14−19] driving PAH synthesis at elevated temperatures of up to a few 1000 K. Supportive electronic structure calculations[18,20−24] and kinetic modeling[14,25−27] suggest that HACA involves a repetitive sequence of atomic hydrogen abstraction from the reacting aromatic hydrocarbon, followed by sequential addition of two acetylene molecules to the radical sites prior to cyclization and aromatization.[12,15,16,20,26,28]

However, in recent years, astronomical observations accompanied by astrochemical models revealed that interstellar PAHs are rapidly destroyed through interstellar shock waves and energetic galactic cosmic rays[29,30] predicting life times of only a few 10^8 years. This contrasts the time scale for the injection of new PAH-based material into the ISM by AGB stars of typically 2×10^9 years. Consequently, the ubiquitous presence of PAHs in the extraterrestrial environments requires further pathways to a rapid formation of PAHs beyond the "established" HACA route. Recently, Parker et al. revealed that naphthalene can be synthesized via the reaction of the phenyl radical (C_6H_5) with vinylacetylene (C_4H_4) via the hydrogen abstraction−vinylacetylene addition (HAVA) reaction pathway. This bimolecular reaction was found to be de facto barrierless and leads via a single, bimolecular gas-phase collision to naphthalene ($C_{10}H_8$) plus atomic hydrogen at temperatures as low as 10 K.[31] However, the phenyl−vinylacetylene system has not been explored at elevated temperatures relevant to circumstellar envelopes of carbon stars of a few thousand kelvins or under combustion-like conditions reaching up to 2000 K. Here the reaction mechanism and branching ratios of the isomers can be quite distinct from 10 K due to a much larger entropy factor and alternative addition routes of the phenyl radical to the carbon atoms of vinylacetylene, which involve entrance barriers. These pathways might be competitive at high temperatures and may lead to non-naphthalene isomers such as phenylvinylacetylenes, thus potentially reducing the yield of naphthalene.

In this Letter, we reveal that the aromatic naphthalene molecule can be synthesized via the reaction of pyrolytically generated phenyl radicals (C_6H_5) with vinylacetylene (HCC−CHCH$_2$; C_4H_4) at elevated temperatures of 1600 K via resonantly stabilized $C_{10}H_{11}$ reaction intermediates exploiting a high-temperature chemical reactor. For distinct structural isomers such as naphthalene and azulene, the adiabatic ionization energies along with the corresponding photoionization efficiency (PIE) curves, which report the intensity of the ion counts at m/z = 128 ($C_{10}H_8^+$) versus the photon energy, are distinct. Therefore, by photoionizing the neutral $C_{10}H_8$ products in a molecular beam by tunable vacuum ultraviolet (VUV) light from the Advanced Light Source (ALS) at various photon energies, we extracted the PIE curve of $C_{10}H_8^+$ at m/z = 128. Through a comparison of these experimentally recorded PIE curves with a linear combination of known reference PIE curves for various $C_{10}H_8$ isomers, naphthalene, 4-phenylvinylacetylene, and *trans*-1-phenylvinylacetylene were found to represent the $C_{10}H_8$ isomers synthesized in the reaction of the phenyl radical with vinylacetylene.

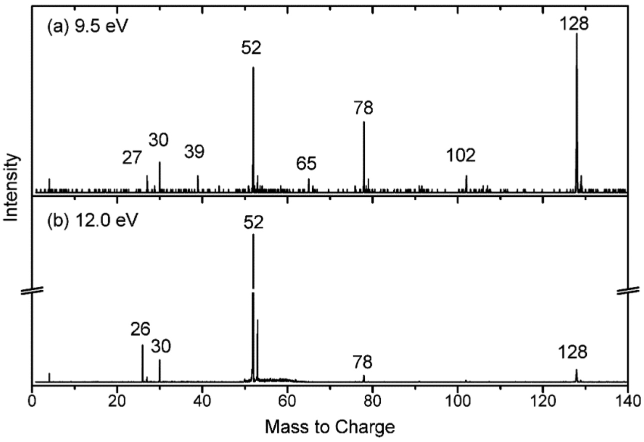

Figure 1. Mass spectra of species in the helium-seeded supersonic beam recorded at photon energies of 9.5 (a) and 12.0 eV (b). Products beyond the $C_{10}H_8$ isomers naphthalene, *trans*-1-phenylvinylacetylene, and 4-phenylvinylacetylene are discussed in the Supporting Information.

Figures 1 and 2 reveal the mass spectra of the species ionized in the supersonic expansion along with the PIE curves of m/z = 128 ($C_{10}H_8^+$) and 129 ($^{13}CC_9H_8^+$) recorded in the phenyl-vinylacetylene system. Figure 2 exhibits the data over a range of photon energies from 8.0 to 9.5 eV along with the PIE reference curves of naphthalene and 4- and *trans*-1-phenylvinylacetylene, together with the overall fit. These data document an excellent match of the experimentally recorded PIE curve at m/z = 128 with a linear combination of the reference curves of three $C_{10}H_8$ isomers. The onset of the ion counts at 8.10 eV agrees exceptionally well with the adiabatic ionization energy of naphthalene of 8.12 eV,[32] whereas the contributions of the additional isomers, in particular, 4-phenylvinylacetylene, become apparent around 8.25 eV. The branching ratios for naphthalene to *trans*-1-phenylvinylacetylene to 4-phenylvinylacetylene were calculated based on the overall fitting of the experimental PIE curve at m/z = 128. All the PIE calibration curves for naphthalene, *trans*-1-phenylvinylacetylene, and 4-phenylvinylacetylene were newly measured in this work, with the photoionization cross sections at 9.5 eV being 23.7, 30.2, and 23.0 Mb, respectively. By linear fitting of these calibration PIE curves to the experimentally measured curve, the branching ratios were extracted to be 43.5±9.0 : 6.5±1.0 : 50.0±10.0%, taking 20% uncertainty in the PIE curves into consideration. It should be noted that the two-ring $C_{10}H_8$ isomer azulene has an adiabatic ionization energy of 7.42 eV[32] and therefore the absence of signal below 8.14 eV clearly indicates the absence of azulene as a reaction product. Also, it is important to highlight that under our experimental conditions, the nitrosobenzene precursor (C_6H_5NO; 107 amu), which is present at a level of 2.6% in the helium-seeded vinylacetylene (5%) beam, decomposes quantitatively to the phenyl radical (C_6H_5) plus nitrogen monoxide (NO).[15,33−35] Likewise,

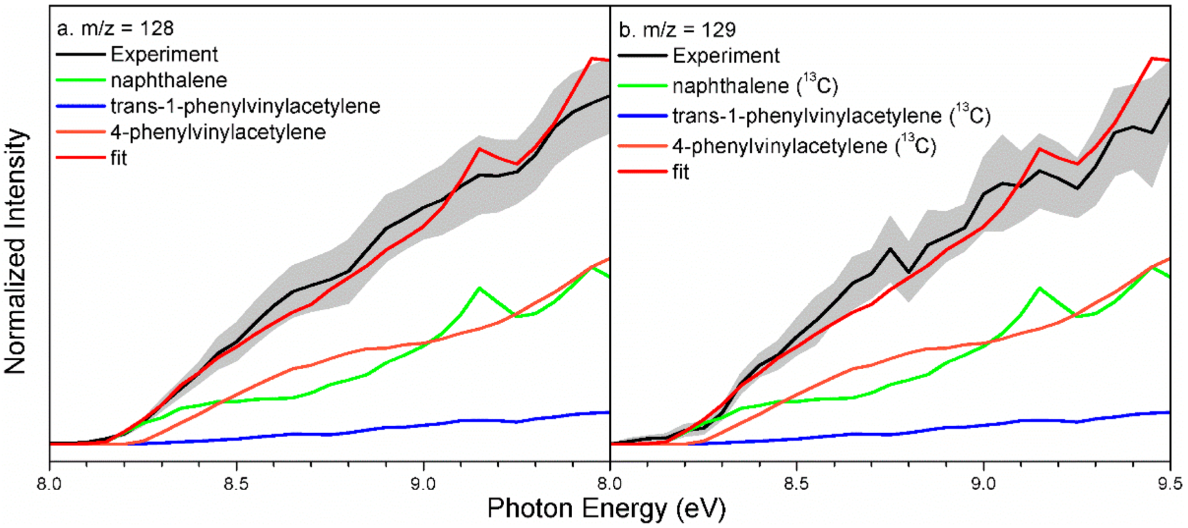

Figure 2. Experimental and reference PIE curves for species at $m/z = 128$ (a) and 129 (b) in the phenyl−vinylacetylene system. The black line refers to the normalized experimental data with 1σ error limits defined in the shaded area; the green, orange, and blue lines show the isomer PIE curves generated by linear fit with measured references PIE curves of naphthalene, 4-phenylvinylacetylene, and *trans*-1-phenylvinylacetylene, respectively. The red line reveals the overall fit via a linear combination of the reference curves.

control experiments in the absence of vinylacetylene do not depict any signal at $m/z = 128$.[33] Therefore, we conclude that the formation of naphthalene and its isomers requires the presence of the phenyl radical and vinylacetylene in the reactor (Supporting Information).

Having identified naphthalene, 4-phenylvinylacetylene, and *trans*-1-phenylvinylacetylene, we are also aiming to elucidate the underlying reaction pathway(s). This requires a close look at the pertinent potential energy surfaces (PESs) and also simulation of the gas flow inside the pyrolytic reactor using the COMSOL package coupled to a kinetics model accounting for the residence time in the heated microreactor of ∼560 μs (Supporting Information). Our recent theoretical study[36] described the PES for the reaction, structures, and molecular properties of all intermediates and transition states involved and temperature- and pressure-dependent rate constants in the phenylvinylacetylene system. The results of the kinetics calculations revealed that under the experimental conditions of the reactor the prevailing products are 4-phenylvinylacetylene (P3) and *trans*-1-phenylvinylacetylene (P2) along with atomic hydrogen with rate constants of 1.4×10^{-12} and 6.6×10^{-13} cm^3 molecule^{-1} s^{-1} and yields, excluding the direct hydrogen abstraction products, of 62 and 31%, respectively. The yields of naphthalene (P1) were computed to be <1% with the rate constant for its formation as low as 1.3×10^{-14} cm^3 molecule^{-1} s^{-1}. Here 4-phenylvinylacetylene is produced via the phenyl radical addition to the C4 acetylenic carbon atom occurring via a barrier of 5 kJ mol^{-1}, followed by the atomic hydrogen loss from the attacked carbon atom (Figure 3). Similarly, *trans*-1-phenylvinylacetylene is formed by phenyl addition to the C1 carbon atom of the vinyl moiety via a submerged barrier located 0.4 kJ mol^{-1} below the reactants. It is important to note that the pathway to naphthalene proceeds through the same submerged barrier and involves two hydrogen shifts and ring closure prior to hydrogen atom elimination; the transition state is lower in energy than the barrier involved in the immediate hydrogen atom loss from the collision complex forming *trans*-1-phenylvinylacetylene. Consequently, the pathway to naphthalene is favorable at low temperatures and pressures. However, this channel does not appear to be competitive at 1600 K in our reactor due to the unfavorable entropic factor. In addition to the $C_{10}H_8$ products, the formation of the direct hydrogen atom abstraction product benzene (C_6H_6) along with distinct C_4H_3 isomers is competitive at 1600 K with rate constants of (5.8 and 3.8) × 10^{-13} cm^3 molecule^{-1} s^{-1} for *i*-C_4H_3 and *n*-C_4H_3, respectively.

How can we explain the predominant formation of naphthalene in the pyrolytic reactor? The aforementioned discussion only accounted for bimolecular collisions and hence the primary reaction products. However, the pressure profile in the reactor, the presence of hydrogen atoms released in the bimolecular reactions, and the residence time also allow for secondary reactions to occur (Supporting Information). Therefore, a detailed kinetic modeling coupled to the gas-flow simulations allows us to reconcile theory and experiment. This model is essential to extract the dominating reactions in the reactor because the conditions such as temperature and pressure along the reactor axis are not homogeneous (Supporting Information). The kinetic reaction scheme includes the quantitative unimolecular decomposition of the reactants such as nitrosobenzene (C_6H_5NO), the primary reactions of the phenyl radical (C_6H_5) with vinylacetylene (C_4H_4), secondary reactions of the hydrogen-assisted isomerization of the $C_{10}H_8$ isomers, and reactions to account for the detection of acetylene (C_2H_2, $m/z = 26$), the vinyl radical (C_2H_3, $m/z = 27$), the propargyl radical (C_3H_3, $m/z = 39$), cyclopentadienyl (C_5H_5, $m/z = 65$), benzene and fulvene (C_6H_6, $m/z = 78$), and phenylacetylene (C_8H_6, $m/z = 102$) with rate constants taken from the literature (Supporting Information).[36−50] Figure 4 illustrates the overall change of the concentration of phenyl (C_6H_5), benzene (C_6H_6), and the $C_{10}H_8$ isomers along the reactor axis. Considering the pyrolysis, the fraction of the phenyl radical manifests a fast growth and rapid drop peaking at the distance where the gas temperature is close to 1100 K. The interval required for the quantitative nitrosobenzene (C_6H_5NO) decomposition along the axis is only 1 mm. From this point, the phenyl radicals start producing initial $C_{10}H_8$ isomers via primary reactions. During the distance

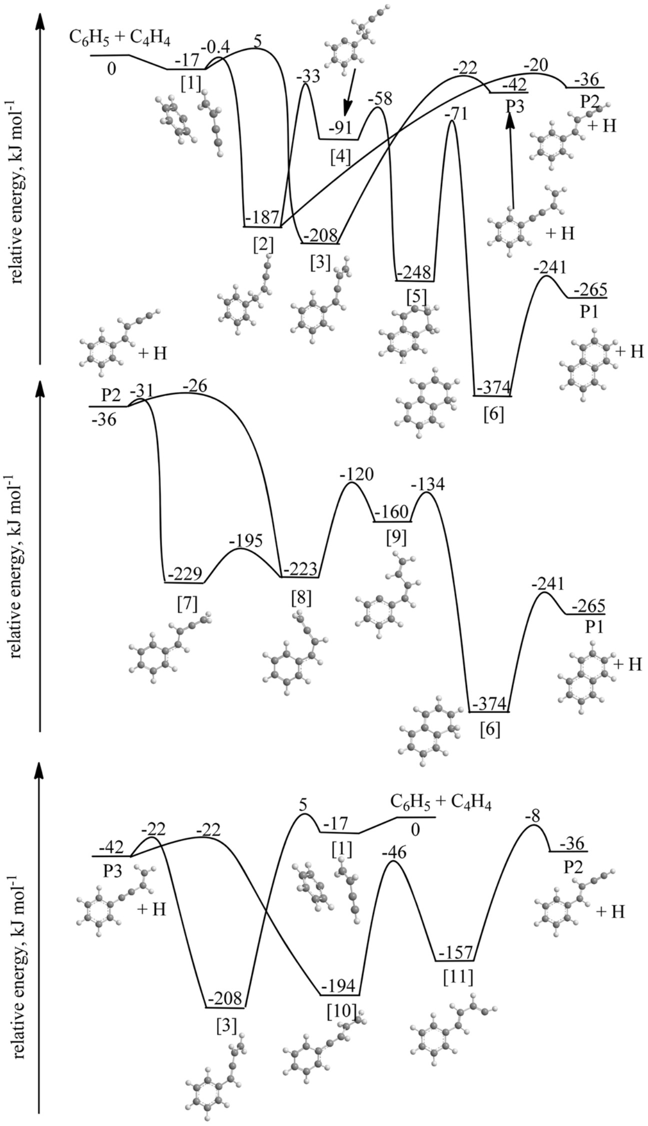

Figure 3. Potential energy surfaces (PESs) for the most favorable channels involved in the formation of three $C_{10}H_8$ isomers within the phenyl−vinylacetylene system via bimolecular reactions (top) and hydrogen-assisted isomerization (center, bottom) based on the calculations from ref 36.

from about 1.2 to 1.5 cm, the fractions of the phenylvinylacetylene isomers (P2, P3) grow much faster than that for naphthalene (P1). Later, P2 and P3 convert to the most stable naphthalene isomer via hydrogen-assisted isomerization (R4) and (R5) (Supporting Information). The transformation of P2 and P3 into P1 occurs in the distances from 1.5 to 2.0 cm and essentially terminates at a distance of 2.0 cm from the entrance of the microreactor. The calculated and experimental molar fractions of P1, P2, and P3 at the exit of the microreactor showed that the experimental conditions are not favorable for the total transformation of P2 and P3 into P1. The incomplete transformation of P2 and P3 into P1 is based on several factors, including a low rate constant of reaction (R5c), a sharp drop of the hydrogen atoms concentration, and the short length of the reactor. Kinetic simulations revealed that a nearly total transformation of P2 and P3 into P1 can be achieved at times >10 ms. This order of magnitude is much larger than the residence time in our reactor. This emphasizes the advantage of the short-length microreactor, allowing us to reveal fine details of the elementary reaction mechanism (primary and secondary reactions), which otherwise would have been masked due to the full conversion of all $C_{10}H_8$ isomers produced initially to naphthalene.

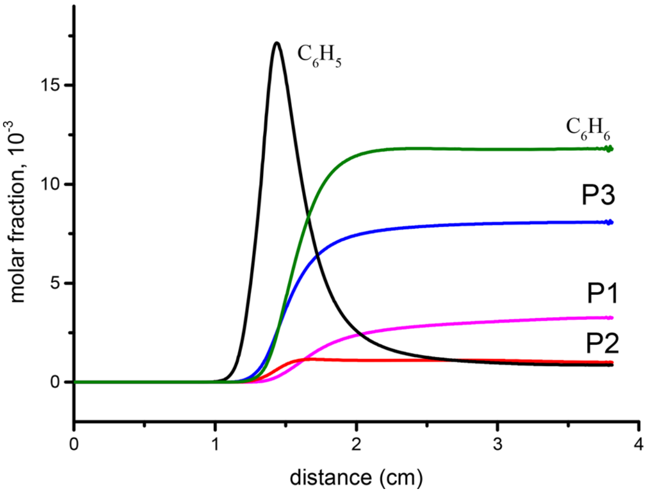

Figure 4. Simulated profiles of the molar fractions of phenyl (C_6H_5) and benzene (C_6H_6) and the $C_{10}H_8$ isomers naphthalene (P1), *trans*-1-phenylvinylacetylene (P2), and 4-phenylvinylacetylene (P3) along the reactor axis.

To summarize, our experiments exploiting a high-temperature chemical reactor revealed that the simplest PAH, naphthalene ($C_{10}H_8$), can be synthesized under combustion-like conditions via a directed synthesis of the phenyl radical reacting with vinylacetylene. Higher energy structural isomers of naphthalene, *trans*-1-phenylvinylacetylene and 4-phenylvinylacetylene, which also form in the reactor, undergo hydrogen-assisted isomerization to the thermodynamically most stable naphthalene molecule during their residence time in the reactor. These pathways are strongly distinct from crossed molecular beams studies of this system,[31] in which the nascent reaction products "fly away" from the reaction center and hence cannot undergo subsequent hydrogen-assisted isomerization reactions. Therefore, crossed molecular beams and pyrolytic reactor studies are highly complementary, leading to the identification of PAHs (naphthalene) along with high-energy isomers synthesized under single collision conditions (crossed beams) together with hydrogen-assisted isomerization products (pyrolytic reactor), ultimately untangling the complex processes and reaction mechanisms of elementary bimolecular reactions, leading to PAHs in combustion systems and in extraterrestrial environments. Furthermore, the combined gas-flow and kinetic simulations of the reactor represent a powerful tool not only for a detailed understanding of the intricate physical and chemical processes inside the high-temperature chemical reactor but also for a quantification and validation of the observed product yields. Future studies of this reactor in combination with electronic structure calculations and kinetics simulations are aimed to systematically unravel mass growth processes via aryl-type radical reactions with acetylene (HACA) and vinylacetylene (HAVA) synthesizing three- and even four-membered PAHs such as anthracene, phenanthrene, and triphenylene. However, whereas PAH formation via HACA only operates at elevated temperatures due to the inherent barriers of aryl radical addition to acetylene, HAVA may operate at temperatures as low as 10 K as well, considering the

DOI: 10.1021/acs.jpclett.8b01020
J. Phys. Chem. Lett. 2018, 9, 2620−2626

defacto barrierless nature of this mechanism. In particular, at very low pressures and in the temperature range from 100 to 200 K, the rate constant for phenyl plus vinylacetylene reaction yielding naphthalene plus atomic hydrogen, (4 to 6) × 10^{-15} cm^3 $molecule^{-1}$ s^{-1}, is from eight to two orders of magnitude higher than the rate constant for the reaction of phenyl radicals with acetylene forming phenylacetylene plus atomic hydrogen, the first step in HACA, and the difference is even higher below 100 K. This can lead to the formation of distinct PAHs in cold molecular clouds via HAVA, which cannot be synthesized via HACA-type mechanisms, thus providing an intimate understanding of the carbon chemistry in the universe.

EXPERIMENTAL METHODS

The experiments were conducted at the ALS at the Chemical Dynamics Beamline (9.0.2) exploiting a high-temperature chemical reactor. In brief, the reactor consists of a resistively heated silicon carbide (SiC) tube of 20 mm length and 1 mm inner diameter. A continuous supersonic beam of phenyl radicals (C_6H_5) was generated in situ via quantitative pyrolysis of nitrosobenzene (C_6H_5NO, TCI-America, >98%, preheated to 323 K) seeded in vinylacetylene/helium carrier gas (5% C_4H_4 in He; Airgas) introduced at a backing pressure of 300 Torr and 1600 K into the silicon carbide tube. Vinylacetylene acts not only as a seeding gas but also as a reactant with the phenyl radical. The residence time of the reactants in the reactor was determined to be near 560 μs (Supporting Information). After exiting the silicon carbide tube, the molecular beam, which contains the reaction products, passes a 2 mm skimmer and enters the detection chamber containing a Wiley−McLaren reflectron time-of-flight (ReTOF) mass spectrometer. The products were then photoionized in the extraction region of the ReTOF by exploiting quasi-continuous tunable VUV synchrotron light and detected with a microchannel plate (MCP). Here mass spectra were taken in the photon energy range from 8.00 to 9.50 eV in steps of 0.05 eV. The PIE curves, which report the intensity of a single mass-to-charge ratio (m/z) versus the photon energy, were extracted by integrating the signal collected at a specific m/z selected for the species of interest over the range of photon energies and normalized to the incident photon flux. The supersonically cooled nature of the beam of the product molecules presents a crucial prerequisite for their detection because the products are rotationally and vibrationally cooled in the expansion.[51] Two naphthalene isomers, 4-phenylvinylacetylene (P3) and *trans*-1-phenylvinylacetylene (P2), were synthesized by Sonogashira cross-coupling reactions (Supporting Information); their PIE curves were recorded via vacuum sublimation of these isomers, recording mass spectra from 8.00 to 9.50 eV in steps of 0.05 eV, and extracting the ion count profiles at m/z = 128.

ASSOCIATED CONTENT

Ⓢ Supporting Information

The Supporting Information is available free of charge on the ACS Publications website at DOI: 10.1021/acs.jpclett.8b01020.

> Description of the synthesis of 4-phenylvinylacetylene and *trans*-1-phenylvinylacetylene including ^1H NMR and ^{13}C NMR spectra of these compounds; description of the modeling procedure of the gas flow and kinetics of the phenyl−vinylacetylene system in the microreactor including the reaction mechanism, physical constants, and reaction rate constants used; and PIE curves and fits of low-molecular-weight products. (PDF)

AUTHOR INFORMATION

Corresponding Authors

*R.I.K.: E-mail: ralfk@hawaii.edu.
*M.A.: E-mail: mahmed@lbl.gov.
*A.M.M.: E-mail: mebela@fiu.edu.

ORCID

Ralf I. Kaiser: 0000-0002-7233-7206
Bo Xu: 0000-0002-1120-3423
Stanislaw F. Wnuk: 0000-0002-3111-3919
Alexander M. Mebel: 0000-0002-7233-3133

Notes

The authors declare no competing financial interest.

ACKNOWLEDGMENTS

This work was supported by the U.S. Department of Energy, Basic Energy Sciences DE-FG02-03ER15411 and DE-FG02-04ER15570 to the University of Hawaii and to Florida International University, respectively. M.A., B.X, U.A. along with the experiments at the Advanced Light Source is supported by the Director, Office of Science, Office of Basic Energy Sciences of the U.S. Department of Energy under contract no. DE-AC02-05CH11231, through the Gas Phase Chemical Physics program, Chemical Sciences Division. The reactor modeling studies at Samara National Research University were supported by Ministry of Education and Science of the Russian Federation (grant no. 14.Y26.31.0020). A.H.H. is the recipient of the Florida International University Presidential Fellowship. We thank Dr. Stephen J. Klippenstein for sharing with us some unpublished rate constants related to reactions on C_4H_5 (H + C_4H_4), C_6H_6, and C_6H_7 (C_4H_5 + C_2H_2) potential energy surfaces used in kinetic modeling.

REFERENCES

(1) Salama, F.; Galazutdinov, G.; Krełowski, J.; Allamandola, L.; Musaev, F. Polycyclic Aromatic Hydrocarbons and the Diffuse Interstellar Bands: A Survey. *Astrophys. J.* **1999**, *526*, 265−273.

(2) Duley, W. Polycyclic Aromatic Hydrocarbons, Carbon Nanoparticles and the Diffuse Interstellar Bands. *Faraday Discuss.* **2006**, *133*, 415−425.

(3) Ricks, A. M.; Douberly, G. E.; Duncan, M. A. The Infrared Spectrum of Protonated Naphthalene and Its Relevance for the Unidentified Infrared Bands. *Astrophys. J.* **2009**, *702*, 301−306.

(4) Schlemmer, S.; Cook, D.; Harrison, J.; Wurfel, B.; Chapman, W.; Saykally, R. The Unidentified Interstellar Infrared Bands: PAHs as Carriers? *Science* **1994**, *265*, 1686−1689.

(5) Bernstein, M. P.; Sandford, S. A.; Allamandola, L. J.; Gillette, J. S.; Clemett, S. J.; Zare, R. N. UV Irradiation of Polycyclic Aromatic Hydrocarbons in Ices: Production of Alcohols, Quinones, and Ethers. *Science* **1999**, *283*, 1135−1138.

(6) Ehrenfreund, P.; Sephton, M. A. Carbon Molecules in Space: From Astrochemistry to Astrobiology. *Faraday Discuss.* **2006**, *133*, 277−288.

(7) Herbst, E.; Van Dishoeck, E. F. Complex Organic Interstellar Molecules. *Annu. Rev. Astron. Astrophys.* **2009**, *47*, 427−480.

(8) Puget, J. L.; Léger, A. A New Component of the Interstellar Matter: Small Grains and Large Aromatic Molecules. *Annu. Rev. Astron. Astrophys.* **1989**, *27*, 161−198.

(9) Schmitt-Kopplin, P.; Gabelica, Z.; Gougeon, R. D.; Fekete, A.; Kanawati, B.; Harir, M.; Gebefuegi, I.; Eckel, G.; Hertkorn, N. High Molecular Diversity of Extraterrestrial Organic Matter in Murchison

Meteorite Revealed 40 Years after Its Fall. *Proc. Natl. Acad. Sci. U. S. A.* **2010**, *107*, 2763−2768.

(10) Tielens, A. G. G. M. Interstellar Polycyclic Aromatic Hydrocarbon Molecules. *Annu. Rev. Astron. Astrophys.* **2008**, *46*, 289−337.

(11) Ziurys, L. M. The Chemistry in Circumstellar Envelopes of Evolved Stars: Following the Origin of the Elements to the Origin of Life. *Proc. Natl. Acad. Sci. U. S. A.* **2006**, *103*, 12274−12279.

(12) Frenklach, M.; Feigelson, E. D. Formation of Polycyclic Aromatic Hydrocarbons in Circumstellar Envelopes. *Astrophys. J.* **1989**, *341*, 372−384.

(13) Cherchneff, I. The Inner Wind of IRC+ 10216 Revisited: New Exotic Chemistry and Diagnostic for Dust Condensation in Carbon Stars. *Astron. Astrophys.* **2012**, *545*, A12.

(14) Wang, H.; Frenklach, M. A Detailed Kinetic Modeling Study of Aromatics Formation in Laminar Premixed Acetylene and Ethylene Flames. *Combust. Flame* **1997**, *110*, 173−221.

(15) Parker, D. S.; Kaiser, R. I.; Troy, T. P.; Ahmed, M. Hydrogen Abstraction/Acetylene Addition Revealed. *Angew. Chem., Int. Ed.* **2014**, *53*, 7740−7744.

(16) Parker, D. S. N.; Kaiser, R. I.; Bandyopadhyay, B.; Kostko, O.; Troy, T. P.; Ahmed, M. Unexpected Chemistry from the Reaction of Naphthyl and Acetylene at Combustion-Like Temperatures. *Angew. Chem., Int. Ed.* **2015**, *54*, 5421−5424.

(17) Parker, D. S. N.; Kaiser, R. I.; Kostko, O.; Ahmed, M. Selective Formation of Indene through the Reaction of Benzyl Radicals with Acetylene. *ChemPhysChem* **2015**, *16*, 2091−2093.

(18) Yang, T.; Kaiser, R. I.; Troy, T. P.; Xu, B.; Kostko, O.; Ahmed, M.; Mebel, A. M.; Zagidullin, M. V.; Azyazov, V. N. HACA's Heritage: A Free-Radical Pathway to Phenanthrene in Circumstellar Envelopes of Asymptotic Giant Branch Stars. *Angew. Chem., Int. Ed.* **2017**, *56*, 4515−4519.

(19) Matsugi, A.; Miyoshi, A. Modeling of Two- and Three-Ring Aromatics Formation in the Pyrolysis of Toluene. *Proc. Combust. Inst.* **2013**, *34*, 269−277.

(20) Richter, H.; Howard, J. B. Formation of Polycyclic Aromatic Hydrocarbons and Their Growth to Soot - A Review of Chemical Reaction Pathways. *Prog. Energy Combust. Sci.* **2000**, *26*, 565−608.

(21) Marsh, N. D.; Wornat, M. J. Formation Pathways of Ethynyl-Substituted and Cyclopenta-Fused Polycyclic Aromatic Hydrocarbons. *Proc. Combust. Inst.* **2000**, *28*, 2585−2592.

(22) Tokmakov, I. V.; Lin, M. C. Reaction of Phenyl Radicals with Acetylene: Quantum Chemical Investigation of the Mechanism and Master Equation Analysis of the Kinetics. *J. Am. Chem. Soc.* **2003**, *125*, 11397−11408.

(23) Kislov, V. V.; Islamova, N. I.; Kolker, A. M.; Lin, S. H.; Mebel, A. M. Hydrogen Abstraction Acetylene Addition and Diels-Alder Mechanisms of PAH Formation: A Detailed Study Using First Principles Calculations. *J. Chem. Theory Comput.* **2005**, *1*, 908−924.

(24) Kislov, V. V.; Sadovnikov, A. I.; Mebel, A. M. Formation Mechanism of Polycyclic Aromatic Hydrocarbons beyond the Second Aromatic Ring. *J. Phys. Chem. A* **2013**, *117*, 4794−4816.

(25) Frenklach, M.; Wang, H. Detailed Modeling of Soot Particle Nucleation and Growth. *Symp. Combust., [Proc.]* **1991**, *23*, 1559−1566.

(26) Bittner, J.; Howard, J. Composition Profiles and Reaction Mechanisms in a Near-Sooting Premixed Benzene/Oxygen/Argon Flame. *Symp. Combust., [Proc.]* **1981**, *18*, 1105−1116.

(27) Wang, H.; Frenklach, M. Calculations of Rate Coefficients for the Chemically Activated Reactions of Acetylene with Vinylic and Aromatic Radicals. *J. Phys. Chem.* **1994**, *98*, 11465−11489.

(28) Appel, J.; Bockhorn, H.; Frenklach, M. Kinetic Modeling of Soot Formation with Detailed Chemistry and Physics: Laminar Premixed Flames of C_2 Hydrocarbons. *Combust. Flame* **2000**, *121*, 122−136.

(29) Micelotta, E.; Jones, A.; Tielens, A. Polycyclic Aromatic Hydrocarbon Processing in Interstellar Shocks. *Astron. Astrophys.* **2010**, *510*, A36.

(30) Jones, A.; Nuth, J. Dust Destruction in the ISM: A Re-Evaluation of Dust Lifetimes. *Astron. Astrophys.* **2011**, *530*, A44.

(31) Parker, D. S.; Zhang, F.; Kim, Y. S.; Kaiser, R. I.; Landera, A.; Kislov, V. V.; Mebel, A. M.; Tielens, A. Low Temperature Formation of Naphthalene and Its Role in the Synthesis of PAHs (Polycyclic Aromatic Hydrocarbons) in the Interstellar Medium. *Proc. Natl. Acad. Sci. U. S. A.* **2012**, *109*, 53−58.

(32) Jochims, H. W.; Rasekh, H.; Ruehl, E.; Baumgaertel, H.; Leach, S. The Photofragmentation of Naphthalene and Azulene Monocations in the Energy Range 7−22 eV. *Chem. Phys.* **1992**, *168*, 159−84.

(33) Zhang, F.; Kaiser, R. I.; Kislov, V. V.; Mebel, A. M.; Golan, A.; Ahmed, M. A VUV Photoionization Study of the Formation of the Indene Molecule and Its Isomers. *J. Phys. Chem. Lett.* **2011**, *2*, 1731−1735.

(34) Zhang, F.; Kaiser, R. I.; Golan, A.; Ahmed, M.; Hansen, N. A VUV Photoionization Study of the Combustion-Relevant Reaction of the Phenyl Radical (C_6H_5) with Propylene (C_3H_6) in a High Temperature Chemical Reactor. *J. Phys. Chem. A* **2012**, *116*, 3541−3546.

(35) Golan, A.; Ahmed, M.; Mebel, A. M.; Kaiser, R. I. A VUV Photoionization Study of the Multichannel Reaction of Phenyl Radicals with 1,3-Butadiene under Combustion Relevant Conditions. *Phys. Chem. Chem. Phys.* **2013**, *15*, 341−347.

(36) Mebel, A. M.; Landera, A.; Kaiser, R. I. Formation Mechanisms of Naphthalene and Indene: From the Interstellar Medium to Combustion Flames. *J. Phys. Chem. A* **2017**, *121*, 901−926.

(37) Park, J.; Dyakov, I. V.; Mebel, A. M.; Lin, M. C. Experimental and Theoretical Studies of the Unimolecular Decomposition of Nitrosobenzene: High-Pressure Rate Constants and the C− N Bond Strength. *J. Phys. Chem. A* **1997**, *101*, 6043−6047.

(38) Horn, C.; Frank, P.; Tranter, R. S.; Schaugg, J.; Grotheer, H.-H.; Just, T. Direct Measurement of the Reaction Pair $C_6H_5NO \rightarrow C_6H_5+$ NO by a Combined Shock Tube and Flow Reactor Approach. *Symp. Combust., [Proc.]* **1996**, *26*, 575−582.

(39) Zador, J.; Fellows, M. D.; Miller, J. A. Initiation Reactions in Acetylene Pyrolysis. *J. Phys. Chem. A* **2017**, *121*, 4203−4217.

(40) Mebel, A. M.; Georgievskii, Y.; Jasper, A. W.; Klippenstein, S. J. Temperature-and Pressure-Dependent Rate Coefficients for the HACA Pathways from Benzene to Naphthalene. *Proc. Combust. Inst.* **2017**, *36*, 919−926.

(41) Miller, J. A.; Klippenstein, S. J.; Robertson, S. H. A Theoretical Analysis of the Reaction Between Vinyl and Acetylene: Quantum Chemistry and Solution of the Master Equation. *J. Phys. Chem. A* **2000**, *104*, 7525−7536.

(42) Knyazev, V. D.; Slagle, I. R. Experimental and Theoretical Study of The $C_2H_3 \rightleftarrows H + C_2H_2$ Reaction. Tunneling and the Shape of Falloff Curves. *J. Phys. Chem.* **1996**, *100*, 16899−16911.

(43) Baulch, D. L.; Cobos, C. J.; Cox, R. A.; Esser, C.; Frank, P.; Just, Th.; Kerr, J. A.; Pilling, M. J.; Troe, J.; Walker, R. W.; et al. Evaluated Kinetic Data for Combustion Modelling. *J. Phys. Chem. Ref. Data* **1992**, *21*, 411−429.

(44) Harding, L. B.; Georgievskii, Y.; Klippenstein, S. J. Predictive Theory for Hydrogen Atom− Hydrocarbon Radical Association Kinetics. *J. Phys. Chem. A* **2005**, *109*, 4646−4656.

(45) Miller, J. A.; Klippenstein, S. J. The Recombination of Propargyl Radicals and Other Reactions on a C_6H_6 Potential. *J. Phys. Chem. A* **2003**, *107*, 7783−7799.

(46) Semenikhin, A. S.; Savchenkova, A. S.; Chechet, I. V.; Matveev, S. G.; Liu, Z.; Frenklach, M.; Mebel, A. M. Rate Constants for H Abstraction from Benzo(a)pyrene and Chrysene: A Theoretical Study. *Phys. Chem. Chem. Phys.* **2017**, *19*, 25401−25413.

(47) Jasper, A. W.; Hansen, N. Hydrogen-Assisted Isomerizations of Fulvene to Benzene and of Larger Cyclic Aromatic Hydrocarbons. *Proc. Combust. Inst.* **2013**, *34*, 279−287.

(48) da Silva, G. Mystery of 1-Vinylpropargyl Formation from Acetylene Addition to the Propargyl Radical: An Open-and-Shut Case. *J. Phys. Chem. A* **2017**, *121*, 2086−2095.

(49) Madden, L. K.; Moskaleva, L. V.; Kristyan, S.; Lin, M. C. Ab Initio MO Study of the Unimolecular Decomposition of the Phenyl Radical. *J. Phys. Chem. A* **1997**, *101*, 6790−6797.

DOI: 10.1021/acs.jpclett.8b01020
J. Phys. Chem. Lett. 2018, 9, 2620−2626

(50) Senosiain, J. P.; Miller, J. A. The Reaction of *n*-and *i*-C_4H_5 Radicals with Acetylene. *J. Phys. Chem. A* **2007**, *111*, 3740−3747.

(51) Vasiliou, A. K.; Piech, K. M.; Reed, B.; Zhang, X.; Nimlos, M. R.; Ahmed, M.; Golan, A.; Kostko, O.; Osborn, D. L.; David, D. E.; et al. Thermal Decomposition of CH_3CHO Studied by Matrix Infrared Spectroscopy and Photoionization Mass Spectroscopy. *J. Chem. Phys.* **2012**, *137*, 164308.

DOI: 10.1021/acs.jpclett.8b01020